

Mineralogical and Geochemical Characterization of Jarash Kaolinitic Clay, Northern Jordan

Talal Al-Momani*, Mohammad Alqudah, "Mohammed-Ezz-Aldien" Dwairi

Yarmouk University, Faculty of Science, Department of Earth and Environmental Sciences, Jordan.

Received 26 January 2020, Accepted 18 June 2020

Abstract

Kaolinite-rich beds occur in Jarash area, northern Jordan. The major chemical components of Jarash kaolinitic clay are SiO_2 , Al_2O_3 and Fe_2O_3 with average values of 61.0% (range = 47.5 - 78.1%), 19.77% (range = 10.8 - 26.33%), 4.58% (range = 1.41 - 10.15%) respectively. Other oxides (K_2O , TiO_2 , CaO , MgO , and MnO) are present as minor components. The low Al_2O_3 and high Fe_2O_3 values indicate a low-grade clay deposit. The XRD results have indicated that kaolinite and quartz are the major mineral constituents, while smectite and muscovite/illite are the minor constituents. The SEM and TEM photomicrographs have indicated that kaolinite is well crystalline with euhedral to subhedral pseudo-hexagonal forms. IR spectroscopy results indicate that the kaolinite is moderate to well crystalline. The thermographs (DTA/TGA results) confirm the thermal behavior of kaolinite as the structure decomposes at $\sim 900^\circ\text{C}$.

The chemical, mineralogical, physical, and technical characteristics of Jarash kaolinitic clay (after attrition and wet sieving) have indicated its possible suitability for pottery, ceramic tiles, and brick-making industries.

© 2020 Jordan Journal of Earth and Environmental Sciences. All rights reserved

Keywords: Clay, Characterization, Kaolinite, Ceramics, Jarash, Jordan.

1. Introduction

Clay minerals constitute about 16% of the total volume of sedimentary rocks on the Earth's surface (Khoury, 2002). The term clay refers to the sediments when consisting of grains the size of less than $2\ \mu\text{m}$ in diameter. The claystone usually consists of a mixture of clay minerals and other rock debris of varying composition (Khoury, 2002; Khoury et al., 2008). Kaolinite, the most common clay mineral, is a 1:1 layered silicate composed of alternating layers of $[\text{Si}_2\text{O}_5]^{2-}$ and $[\text{Al}_2(\text{OH})_4]^{2+}$. The theoretical formula of kaolinite is $\text{Si}_2\text{Al}_2\text{O}_5(\text{OH})_4$ (frequently expressed as $\text{Al}_2\text{O}_3 \cdot 2\text{SiO}_2 \cdot 2\text{H}_2\text{O}$). Kaolin deposits contain kaolinite together with other clay minerals, e.g., smectite and illite (Correia et al., 2005).

Clays have played a very important role in the industrial technology in recent years; kaolinite is one of the most important and widely-distributed clay minerals (Murray 2007; Dominguez et al., 2016; Abu Yaya et al., 2017; Kharbush and Farhat, 2017). The outstanding chemical and physical properties of kaolinite enable its use in agricultural, engineering, and construction industries. Kaolinite is used as an important commodity in ceramic, paper, plastic, rubber, cement, clay bricks, geopolymers, paint, cosmetic, and many other industries (Ciullo, 1996; Murray 2007; Al Ani and Sarapaa, 2008; Attah and Oden, 2010; Kashcheev and Turlova, 2010; Khoury 2019).

Kaolinite is used in many applications such as paper filling and coating (45 %), refractories and ceramics (31

%), fiberglass (6 %), cement (6 %), rubber and plastic (5 %), paint (3 %), and other industries (4 %) (Eletta et al., 2015). Technological properties of ceramic products depend on the physical, chemical, and mineralogical characteristics of the starting raw materials, which also control the overall processing before firing (Correia et al., 2005).

In Jordan, kaolinite-rich beds occur in Mahis, Ghor-Kabid, Batn El-Ghoul, and Hiswa areas (Khoury 2002; 2006). The Jordanian kaolinite was characterized by many authors (i.e. Khoury and El-Sakka, 1986 ; Al-Momani, 2000, 2008; Qtaitat and Al-Trawneh 2005; Al-Momani and Khoury, 2010; Gougazeh and Buhl 2010; Al-Momani and Dwairi, 2018; Khoury 2002; 2019). Kaolinite is used in the cement industry, ceramics (sanitary ware and tiles, artistic ceramic ware, table-ware kitchen-ware, and stone-ware (pipes and tiles). The estimated kaolin reserves in various areas in Jordan are as follows: Batn el-Ghoul (2200 Mt), Al-Mudawwara (9700 Mt), Al-Hiswa (54 Mt), and Jabal Umm Sahn and Dubaydib (1090 Mt) (Yasin and Ghannam, 2006).

The geology (sedimentology, paleogeography, structures, mineralogical and engineering behavior of some clay) and depositional environments of Jarash kaolinitic clay were investigated by many authors (Amireh 1994; Ahmad et al., 2012; Abu Hamad et al., 2016).

The following work aims for the first time to characterize and investigate the possible industrial use of the clay deposits in Jarash, northern Jordan.

* Corresponding author e-mail: talalmom@yu.edu.jo

2. Geological Setting of the Study Area

Jarash clay deposits belong to the Early Cretaceous Kurnub Group of Jordan (Table 1) that crops out in many sites of Jordan including the studied area. In northern Jordan, the Kurnub Group (KG) is subdivided into three formations; Ramel, Jarash, and Bir Fa'as from base to top (Amireh and Abed, 1999; Amireh, 2000).

Amireh (1994) used heavy and clay minerals as an effective tool for solving stratigraphic problems. The heavy and clay minerals have been applied on the Kurnub Sandstone (Early Cretaceous) of Jordan. Ahmad et al. (2012) performed a palynological study on the Early Cretaceous

Kurnub Sandstone Formation from Mahis area, central Jordan. Their data was correlated with Abu Hamad et al. (2016) results from the Jarash Formation (Aptian–Albian, Kurnub Group) of northern Jordan.

Figure (1) illustrates the geology of the studied area. Jarash clay deposits belong to the Lower Cretaceous Sandstone (Aptian-Albian age) which consists mainly of clastic sedimentary rocks including dominant sandstones with intercalation of claystones (Amireh, 1997; Abdelhamid, 1995). The studied claystones in the Jarash area are intercalated within the sandstone layers of the Jarash Formation.

Table 1. General Stratigraphy of the Kurnub Group and Jarash Formation in the studied area (Amireh and Abed, 1999).

Era	Period	Series	Group	Formation	Age
Mesozoic	Cretaceous	Upper Cretaceous	Ajliun Group	Na'ur	Turonian
				Bir Fa'as	Cenomanian
		Lower Cretaceous	Kurnub Group	Jarash	Albian
				Ramel	Aptian

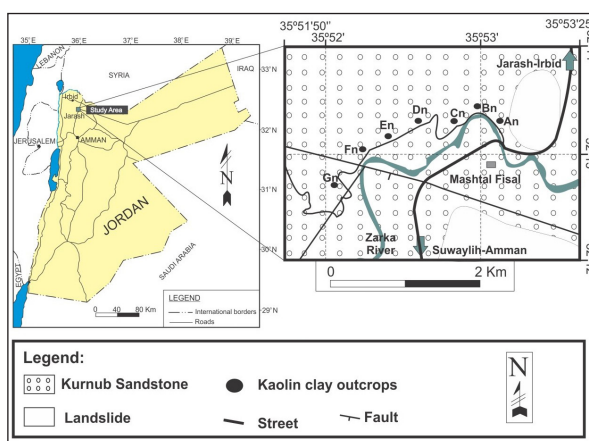


Figure 1. Geological map of the studied area (Modified from Sawariah and Barjous, 1993; Royal Jordanian Geographic Center, 2003).

3. Methodology

Field-work and sampling were carried out during summer 2015 and have focused on the Jarash clay deposit that is located 38 km to the south of Irbid city and around 45 km to the north of Amman city. The site coordinates are 32° 12' 00" N – 32° 14' 00" N and 35° 51' 50" E – 35° 53' 25" E (Figure 1).

110 representative samples were collected from the clay outcrops [seven bulk samples before and after attrition and wet sieving; ninety-six from the different seven outcrops (An, Bn, Cn, Dn, En, Fn, and Gn)]. Attrition and wet sieving were carried out for the bulk samples.

The attrition scrubbing can be referred to as the first step of the wet sieving. The main objective of this process is to separate the fine particles by water and to increase the scoring action of the coarse particles with each other (Preston and Tatarzyn, 2013). Wet sieving was used to separate the fine particles from the coarse particles and to eliminate the major impurities (Bloodworth et al., 1993; Sandgren et al., 2015).

Laboratory attrition scrubber model (IKA-Werk TR-50) was used in this study. The wet sieving was done according to the method of (Bloodworth et al., 1993), British Geological Survey.

Characterization of the clay samples has included detailed chemical analyses for major and trace components using X-ray fluorescence (XRF) and Inductively-coupled plasma (ICP-AES) techniques, mineralogical analysis using X-Ray diffraction (XRD), Infrared Spectroscopy (IR), Scanning electron microscopy (SEM), Transmission electron microscope (TEM), differential thermal (DTA), differential thermogravimetric (DTG) and thermogravimetric analyses (TGA) techniques.

The X-ray fluorescence (XRF) was used in the analysis of the major oxides (Si, Al, Fe, Ti, Mg, Ca, Mn, Na, K, P) using Bruker axs XRF-S4. The samples were analyzed at the laboratories of the Ministry of Energy and Mineral Resources – Amman. A 0.7 gm of each powdered sample was weighted in a clean platinum crucible. Each sample was mixed with 7 gm of flux [1 part Li – tetra borate and 4 parts Li – Meta borate] then was fused in a platinum crucible at 1200°C for five minutes using a standard burner. After cooling, glass discs were used for major elemental analysis.

Fourteen bulk representative samples were analyzed for their trace elements' content (Be, B, Ba, Cd, Co, Cr, Cu, Li, Mo, Nb, V, Pb, Sn, Sr, Y, Zr, Bi, As and W) using Quantima ICP – AES.

Bruker D4 ENDEAVOUR diffractometer with Cu α radiation ($\lambda = 1.5418$) and a scan rate speed of 2°/min at 40 kV and 30 mA were used to obtain the X-ray diffractograms for the whole rock samples that were scanned from 2° - 65° 2 θ . The oriented clay samples were scanned from 2° - 30° 2 θ for untreated, glycolated and heated (550°C) preparations following the procedure of (Poppe et al., 2001, Hutchison, 1974).

Undisturbed clay samples (5 to 10 mm in length) were prepared for SEM analysis. The samples were coated with gold to produce clear and high resolution images (Welton, 2003). FEL-Quanta 200 instrument was used with a magnification range from 1000 to 30,000X (5000X to 20,000X was the most useful).

A transmission electron microscope (TEM) (ZEISS EM 10 TR) was used. TEM micrographs usually give information about the shape, size, and the arrangement of the particles. It also gives more detailed information on the crystallographic and the compositional nature of the particle (William and Carter, 2009). Fifteen representative samples were prepared by dispersing a small portion of the <63 μm fraction using an ultrasonic device. A small amount of this dispersed material was sprayed onto grids, and was supported by a thin carbon film, dried, and mounted in the microscope.

The IR spectroscopy is usually used to focus on the degree of crystallinity of kaolinite (Djomogue and Njopwovo, 2013; Johnston, 2017; Klopogge, 2017; Madejová, et al., 2017). Potassium Bromide (KBr) pellets after wet sieving were prepared for seven representative samples using FT-IR (Bruker FT-IR- 4100) instrument over the range of 400 to 4000 cm^{-1} .

Thermal analyses are used to study the properties of the materials as a result of changing in temperature. In addition, mass change, phase diagrams, and thermal capacity can be obtained through these analyses. The differential thermal analysis (DTA) gives information about endothermic or exothermic reactions. The endothermic reaction describes desorption of surface H_2O , dehydration at low temperature and dehydroxylation at 550°C. On the other hand, crystallization through exothermic reaction takes place at high temperature (>900°C) to form mullite. The thermogravimetric analysis (TGA) determines the mass change with the increase of temperature (Guggenheim and Koster, 2001). The DTA, DTG, and TGA analyses were made using NETZSCH STA 409 PG/PC.

4. Results and Discussion

4.1. XRF Results before and after Attrition and Wet Sieving

The XRF results of the seven bulk samples are given in Table (2). The SiO_2 , Al_2O_3 , Fe_2O_3 , and LOI are the major components, while TiO_2 , K_2O , MnO , MgO , CaO , P_2O_5 are relatively minor components. SiO_2 and Al_2O_3 are usually the main chemical constituents of kaolinite, quartz, and illite. The XRF results after attrition and wet sieving (<63 μm) for all of the samples are also given in Table (2).

Table 2. Maximum, minimum, and average values (wt. %) of the major oxides before and after attrition and wet sieving of the seven bulk Jarash clay samples.

Oxides (wt.%)	Minimum Value		Maximum Value		Average Value		Standard Deviation	
	Before	After	Before	After	Before	After	Before	After
SiO_2	62.5	47.5	85.13	78.60	73.75	61.00	7.22	7.07
TiO_2	0.72	1.06	1.77	2.33	1.303	1.75	0.30	0.25
Al_2O_3	7.54	10.8	20.70	26.33	12.69	19.77	4.10	3.79
Fe_2O_3	1.30	1.41	5.17	10.15	2.912	4.58	1.25	1.74
MnO	0.00	0.00	0.1	0.058	0.008	0.006	0.025	0.01
MgO	0.15	0.24	0.83	1.16	0.293	0.59	0.163	0.23
CaO	0.11	0.21	1.49	10.3	0.720	1.22	0.491	1.46
Na_2O	0.00	0.00	0.18	1.78	0.029	0.058	0.05	0.22
K_2O	0.00	0.05	1.46	1.88	0.864	1.27	0.34	0.20
P_2O_5	0.03	0.029	0.08	0.21	0.044	0.09	0.014	0.004
LOI	3.00	4.4	8.00	16.6	5.54	9.35	1.374	2.20

Table 2 shows that the trend for major oxides' readings before and after wet sieving and attrition. Silica is the highest value, followed by alumina and iron oxides. The table shows also that silica has decreased, and alumina and iron oxides have increased after wet sieving and attrition.

Increased iron content in the clay-rich fraction indicates the presence of iron oxides as fine-grained particles (Jovanovic and Mujkanovic, 2013). Iron oxide (Fe_2O_3) in the clay fraction is detrimental to the clay's effective performance as a refractory material; it then became imperative to reduce

it to an acceptable level of less than 1% by leaching with oxalic acid (Al-Momani 2008; Abd El-Raheem et al., 2009; Florunso et al., 2014).

Correlation Coefficient matrix for the major oxides is given in Table (3). This Table exhibits a high negative correlation between Al_2O_3 and SiO_2 (-0.77), Fe_2O_3 and SiO_2 (-0.81), and LOI and SiO_2 (-0.84). A high positive correlation between LOI and Al_2O_3 (0.73) indicates its relation to kaolinite.

Table 3. Correlation Coefficient matrix for the major oxides in the (96) representative Jarash clay samples. Correlation is significant at the 0.05 level.

	SiO ₂	Al ₂ O ₃	Fe ₂ O ₃	TiO ₂	Na ₂ O	K ₂ O	MnO	MgO	CaO	P ₂ O ₅	LOI
SiO ₂	1	-0.77	-0.81	-0.42	0.19	-0.40	-0.44	-0.47	0.36	-0.27	-0.84
Al ₂ O ₃		1	0.42	0.43	-0.39	0.41	-0.77	0.41	-0.33	0.36	0.73
Fe ₂ O ₃			1	0.26	0.006	0.28	0.52	0.50	-0.32	0.20	0.70
TiO ₂				1	-0.544	0.27	0.083	0.081	-0.221	0.17	0.35
Na ₂ O					1	-0.71	0.060	-0.003	0.203	-0.17	-0.15
K ₂ O						1	0.080	0.341	-0.100	0.17	0.42
MnO							1	0.065	-0.30	0.062	0.19
MgO								1	0.260	0.48	0.71
CaO									1	-0.047	0.011
P ₂ O ₅										1	0.52
LOI											1

4.2. ICP Results

The ICP results of the trace elements for the bulk samples before and after attrition and wet sieving (grain size <63µm) are given in Table (4).

Table 4. Minimum, maximum, average (ppm), and standard deviation values for the different trace elements before and after attrition and wet sieving.

Trace Element (ppm)	Minimum		Maximum		Average		Standard Deviation	
	Before	After	Before	After	Before	After	Before	After
As	77	69	360	276	186	165	244.7	86.03
B	57	41	100	128	70	82	14.4	26.2
Ba	166	197	245	266	206	229	29.9	27.6
Be	2	3	3	3	3	3	0.577	0.0
Bi	ND	ND	ND	ND	ND	ND	ND	ND
Cd	1	3	32	9	16.3	6	22.13	4.24
Co	5	1	73	12	28	8	30.43	4.65
Cr	82	89	125	193	98	156	13.9	40.3
Cu	3	2	8	10	4	3	2.24	2.66
Li	18	31	55	67	35	48	13.1	13.9
Mo	ND	ND	ND	ND	ND	ND	ND	ND
Nb	7	22	59	71	33	43	20.42	19.4
Pb	17	20	119	168	55	100	44.7	74.73
Sn	9	24	169	79	78	52	60.75	27.54
Sr	137	154	300	386	217	274	61.7	72.15
V	77	91	118	149	93	120	16.3	20.7
W	47	34	64	116	55	66	12.02	35.1
Y	30	32	44	54	36	43	4.99	7.71
Zr	232	258	1249	483	568	351	433.9	83.6

(ND: Not Detected).

Some trace elements are enriched in the original samples, and could be incorporated in the non-clay heavy minerals. Other trace elements are enriched in the fine fraction (<63 µm), and could be incorporated in the structure of the clay minerals (Khoury, 2002). The results of trace elements in the Jarash clay samples after wet sieving (<63µm) show that Zr > Sr > Ba > As > Cr > V > Pb > B > W < Sn > Li > Nb > Y > Co > Cd > Cu > Be. The <63µm size fraction indicates

a relatively high concentration of Zr (Average 568 and 351 ppm before and after attrition and wet sieving) that could be related to detrital zircon.

Trace elements are a significant factor in coloring the clay industrial products, and could have a negative impact on the environment through the accumulation of toxic elements in plants, water, and soils (Hou and Jones, 2000).

4.3. X-ray Diffraction (XRD)

The results of X-ray diffraction analysis of the samples before attrition scrubbing and wet sieving indicate that quartz and kaolinite are the most abundant minerals in all the samples. The strongest (highest) peaks for quartz appear at d-spacings=3.34 Å ($2\theta=26.67$) and 4.26 Å ($2\theta=20.85$). Kaolinite major peaks appear at d-spacings 7.17 Å ($2\theta=12.34$) and 3.58 Å ($2\theta=24.88$). Muscovite/illite, calcite, and smectite are found as minor constituents.

Typical oriented XRD clay results for the normal (air dried), glycolated, and heated at 550 °C preparations are illustrated in Figure (2). Kaolinite is characterized by two basal reflections: (001) and (002). The first reflection appears at 7.15 Å, the second one appears at 3.56 Å. Kaolinite reflections are not affected by glycolation, but they disappear upon heating to 550 °C.

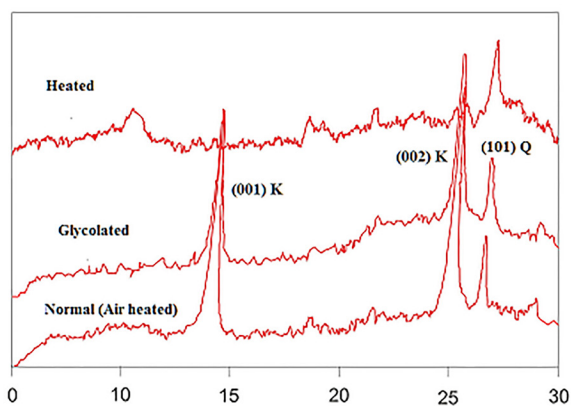


Figure 2. Typical oriented XRD patterns for air-dried, glycolated, and heated to 550 °C sample (Dn2). The number between the brackets indicates hkl reflections. (K: Kaolinite and Q: Quartz).

4.4. Scanning Electron Microscope (SEM)

The crystal shape, texture, and morphology of kaolinite from Jarash clay is obtained from the SEM micrographs as illustrated in Figure (3). Kaolinite is well crystalline with an euhedral pseudo-hexagonal form, and its particle size ranges between 1 and 4 μm.

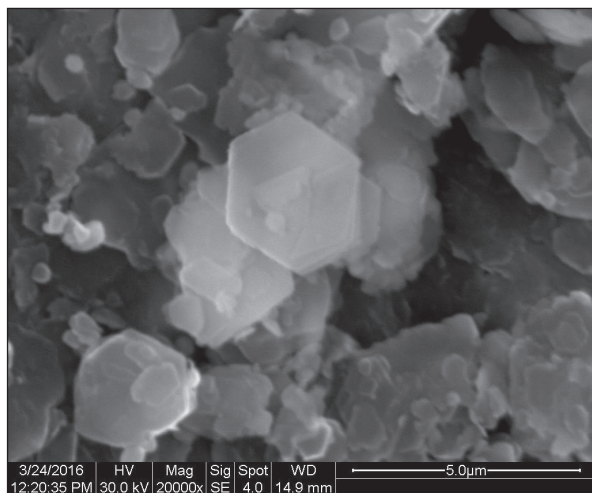


Figure 3. A representative SEM micrograph of pseudo-hexagonal kaolinite from Jarash clay (20000X) (Sample No. Fn1).

4.5. Transmission Electron Microscopy (TEM)

Kaolinite has a pseudo-hexagonal form (euhedral to subhedral) with a particle size that ranges between 200 and 300 nm. Figure (4) shows a typical TEM micrograph of the Jarash kaolinite.

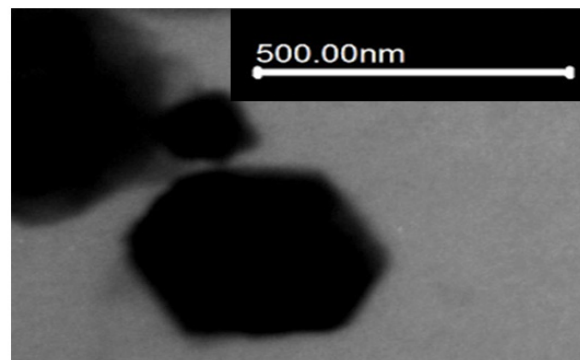


Figure 4. Transmission electron micrograph of well-crystalline pseudo-hexagonal kaolinite from Jarash clay deposit (Sample No. Bn2).

4.6. Infrared Spectroscopy (IR)

Theoretical kaolinite shows high-intensity absorption peaks at 3694, 3650, 3620, 1114, 1032, 1010, 936, 912, 790, 752, 693, 537, 468, 430 cm⁻¹ Ekosse (2005).

Kaolinite [Al₂Si₂O₅(OH)₄] is made up of four well-resolved absorption bands of the hydroxyl group (OH-) which are located at 3695 cm⁻¹, 3670 cm⁻¹, 3650 cm⁻¹, and 3620 cm⁻¹. The high frequency bands are located at 3670 cm⁻¹ and 3695 cm⁻¹, the medium frequency is at 3950 cm⁻¹, while the low-frequency bands are located at 3620 cm⁻¹, 3670 cm⁻¹, 3695 cm⁻¹ and 3650 cm⁻¹, due to the vibration of the external hydroxyls, through the 3620 cm⁻¹ which is described as the inner hydroxyls (Vaculikova et al., 2011; Madejová, et al., 2017).

Infrared spectroscopy (IR) results of selected samples after attrition and wet sieving (< 63 μm) are illustrated in Figure (5). The figure shows a high-intensity absorption band at 3699.99 cm⁻¹ and at 3620.02 cm⁻¹, medium intensity peak at 1618.04 cm⁻¹, and low intensity peaks at 1031.42 cm⁻¹, 912.92 cm⁻¹, and at 469.41 cm⁻¹ that indicate a moderate to well crystalline kaolinite when compared to Vaculikova et al. (2011) and Madejová, et al. (2017).

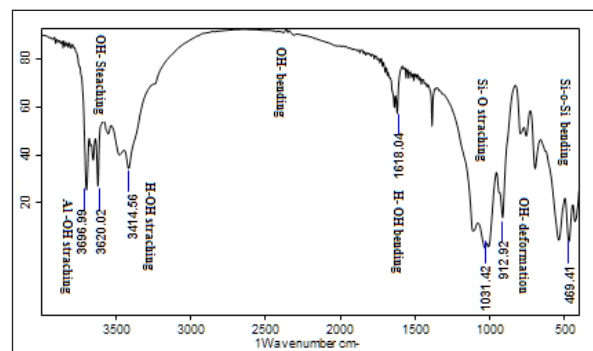


Figure 5. Infrared absorption spectra of Jarash clay from 400 to 4000 cm⁻¹ after attrition and wet sieving (Sample An15).

4.7. DTA-TG Analyses

The DTA results of Jarash clay have indicated that kaolinite is the major clay component. Figures (6 and 7) show the first endothermic peaks range from 150°C to 200°C. The main dehydroxylation endothermic peaks ranges from 500°C to 550°C that indicate the decomposition of kaolinite. A small exothermic peak appears at a range from 880°C to 940°C that is related to the recrystallization process.

The DTG and TG results are illustrated in Figures (6 and 7). It indicates a total loss in weight that ranges from 8 % to 18 %, and is related to dehydration and dehydroxylation. The loss of weight as a result of dehydroxylation of pure kaolinite is 14 % (Eslinger and Peaver, 1988). The dehydroxylation of Jarash clay ranges from 5 % to 9.5 % which means that the samples include other minerals as quartz.

The dehydroxylation process of kaolinite occurs at temperatures ranging from 400 to 700°C, Table (5) (Kakali et al., 2001; Erdemoğlu et al., 2020).

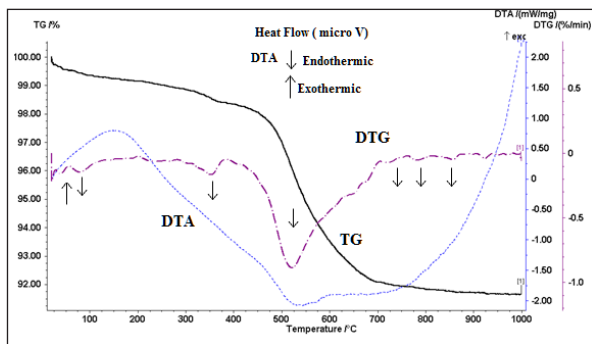


Figure 6. Typical thermal curves (DTA, TG, and DTG) for Jarash clay. (Heating rate = 20°C /min).

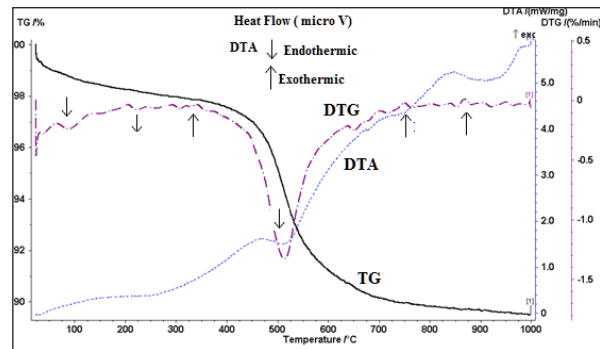


Figure 7. Typical thermal curves (DTA, TG, and DTG) for Jarash clay (Heating rate= 20°C /min).

The XRD, SEM, TEM, IR, DTA and TGA results confirm that the kaolinite of Jarash clay is well crystalline and the (< 63 µm) size fraction is mixed with quartz as a non-clay mineral.

4.8. Possible Industrial Applications

Table (6) summarizes the main chemical constituents of kaolinite deposits of Jordan including this study. Table (7) is a comparison between the average chemical composition of Jarash clay and some selected clay deposits around the World.

Table 5. Thermal transformation stages of kaolinite.

Mineral	Temperature	Thermal transformation phase	Reference
Kaolinite	T<100°C	Low temperature release of absorbed water in pores, on the surfaces.	Kakali et al. (2001)
Kaolinite	100<T<400°C	Weight loss that can be correlated with a pre-dehydration process.	Kakali et al. (2001)
Kaolinite	T<400°C	Removal of surface, pore, and adsorbed water	Erdemoğlu et al. (2020)
Kaolinite	400<T<650°C	Dehydroxylation of kaolinite	Kakali et al. (2001)
Kaolinite	400°C<T<700°C	Dehydroxylation	Erdemoğlu et al. (2020)
Kaolinite	T = ~1000°C	Crystallization of mullite	Kakali et al. (2001)
Kaolinite	T = ~1000°C	Formation of mullite phase and amorphous SiO ₂	Erdemoğlu et al. (2020)
Kaolinite	T >1200°C	Crystallization of cristobalite from amorphous SiO ₂	Erdemoğlu et al. (2020)

Table 6. Chemical composition of kaolinite clay deposits of Jordan (Alshaaer et al., 2002; Khoury, 2002; Yasin and Ghannam, 2006; AL-Momani, 2008; AL-Momani and Khoury, 2010; present study).

Area	Al ₂ O ₃ %			SiO ₂ %			Fe ₂ O ₃ %		
	Min.	Max.	Aver.	Min.	Max.	Aver.	Min.	Max.	Aver.
Batn El-Ghoul	14.01	25.37	19.30	47.79	68.32	56.66	4.05	8.37	7.33
Al-Mudawwara	13.36	27.54	18.97	41.87	70.20	54.95	4.54	10.54	7.91
Al-Hiswa	15.62	28.96	19.25	46.60	66.47	58.73	1.38	9.58	9.15
Jabel Umm Sham and Dubaydib	17.00	24.70	22.52	49.04	61.67	51.50	3.50	11.04	5.52
Jarash Clay (Present Study)	10.8	26.33	19.77	47.5	78.60	61.00	1.14	10.15	4.58

Table 7. Average chemical composition of Jarash clay deposits compared with other clay deposits around the world (wt %).

Oxide (wt. %)	This study	Other Kaolinite deposits in the world			
		Italy	Nigeria	Jordan	Typical chemical composition of clay materials for ceramic tiles from different countries. (AL-Momani, 2000)
		I	II	III	
SiO ₂	61.00	65.43	60.21	58.73	44.9 - 70.0
Al ₂ O ₃	19.77	19.61	19.05	19.25	19.61 - 32.0
Fe ₂ O ₃	4.58	5.72	3.78	9.15	0.5 - 8.6
TiO ₂	1.75	0.59	--	0.83	0.0 - 1.4
Na ₂ O	0.06	0.48	0.42	0.09	0.0 - 1.0
K ₂ O	1.27	1.3	2.16	1.39	0.5 - 1.98
MnO	0.006	--	0.02	0.04	--
MgO	0.59	0.15	1.50	0.16	0.05 - 1.96
CaO	1.22	0.16	0.30	0.05	0.0 - 1.0
P ₂ O ₅	0.09	--	--	0.083	--
LOI	9.35	6.39	10.2	9.36	7.5 - 13.6

I. Clay from Sardinia Italy (Ligas et al., 1997).

II. Ibero and Oboro clay deposits in Nigeria (Mark, 2010).

III. Hiswa clay Kaolin A3 (AL-Momani, 2000; AL-Momani, 2008; AL-Momani and Houry, 2010).

It is noted from Table (6) that the average concentration of aluminum oxide (Al₂O₃%) in the Jarash clay is higher than other different regions (Batn El-Ghoul, and Jabel Umm Sham and Dubaydib), with the exception of Al-Mudawwara and Al-Hiswa clay. In Jarash clay, the average silica oxide (SiO₂%) is higher and the iron oxide (Fe₂O₃%) is lower than other different regions (Al-Mudawwara and Jabel Umm Sham and Dubaydib).

The chemical composition of the Jarash clay deposits as indicated in Table (7) suggests its use as a raw material for refractories or ceramic (Al-Momani, 2000; Mark, 2010) and for the manufacture of vitrified tiles (Ligas et al., 1997; Al-Momani, 2000)

The chemical composition is consistent with those results obtained in a previous work on the physical and technical characteristics of the Jarash clay deposits (Al-Momani and Dwairi, 2018). The authors concluded that the

bulk samples of Jarash clay after the attrition and wet sieving were plotted graphically in the region of the kaolinite, while some samples were plotted in the region of the plastic kaolin (Figure 8). Plastic kaolinite may be affected by the variations of liquid limit (LL), plastic limit (PL), and plasticity index (PI) in the different samples of Jarash clay. Using the clay workability sheet of Bain and Highly (1978), most of the bulk samples of Jarash clay fall within the region of optimum molding properties, and acceptable molding properties which indicate that Jarash clay is suitable for pottery, and brick-clay industry (Figure 9). In addition, the physical characteristics (whiteness, bulk density, and oil absorption), chemical characteristics, technical characteristics [liquid limit (LL), plastic limit (PL), and plasticity index (PI)] of Jarash clay after the attrition and wet sieving endorse that Jarash clay deposits is suitable for pottery, ceramic tiles, and brick-making industries (Table 8).

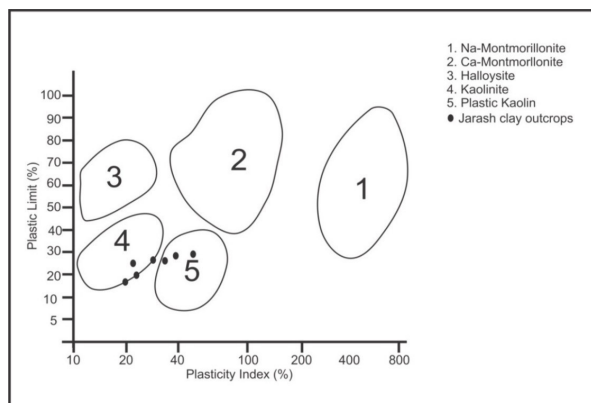


Figure 8. Clay identification for bulk samples after wet sieving and attrition for Jarash clay (<63µm) (Al-Momani and Dwairi, 2018).

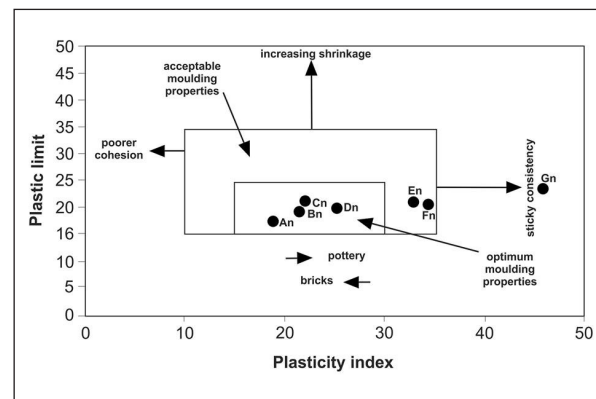


Figure 9. Clay workability chart for samples after wet sieving and attrition (<63 µm) (Al-Momani and Dwairi, 2018).

Table 8. Comparison between the typical chemical properties of clay materials for ceramic tiles.

The Present Study		Mark (2010)	AL-Momani, (2010)	Typical chemical composition of clay materials for ceramic tiles from different countries. (AL-Momani, 2000)	
Chemical composition (wt. %)					
SiO ₂ %	61.00	60.21	58.73	44.9 - 70.0	
Al ₂ O ₃ %	19.77	19.05	19.25	19.61 - 32.0	
Fe ₂ O ₃ %	4.58	3.70	9.15	0.5 - 8.6	
TiO ₂ %	1.75	--	0.83	0.0 - 1.4	
Na ₂ O%	0.06	0.42	0.09	0.0 - 1.0	
K ₂ O%	1.27	2.16	1.39	0.5 - 1.98	
MnO%	0.006	--	0.04	--	
MgO%	0.59	1.50	0.16	0.05 - 1.96	
CaO%	1.22	0.30	0.05	0.0 - 1.0	
P ₂ O ₅ %	0.09	-	0.08	--	
LOI	9.35	10.2	7.14	7.5 - 13.6	
Technical properties					
Plastic limit (Wt. %)	Range	15.9 - 26.3	19.0	18.09	16.0 – 26.0
	Average	19.74			
Liquid limit (Wt. %)	Range	34.2 - 71.5	42.4	30.05	23.0 – 42.0
	Average	48.18			
Plasticity index (Wt. %)	Range	18.3 - 45.2	23.0	11.96	9.0 – 26.6
	Average	19.74			
Physical properties					
Bulk Density (g/cm ³)	Range	0.86 - 1.22	1.66	0.69-1.33	
	Average	0.99			
Oil Absorption (g/100g)	Range	23.35 - 46.5	--	21.81-35.34	
	Average	33.1			

5. Conclusions

XRD, SEM, TEM, IR, DTA, DTG, and (TGA) results have confirmed that kaolinite is the major Jarash clay mineral constituent together with quartz. Small amounts of muscovite/illite and smectite are also present. Kaolinite of Jarash clay is well crystalline with a pseudo-hexagonal form and a crystal size that ranges between 1 and 4 µm.

The overall chemical results are comparable with other clay deposits in Jordan (Batn el-Ghoul, Al-Mudawwara, Al-Hiswa) and other countries (Nigeria and Italy).

The chemical, mineralogical, physical, and technical characteristics of Jarash clay after the attrition and wet sieving suggest its use in pottery, ceramic tiles, and brick-making industries.

Processing and treatment of Jarash clay should be used to increase the Al₂O₃ and reduce the Fe₂O₃ contents which can be achieved by different methods such as chemical leaching in order to meet the specifications of other ceramic industries.

Acknowledgements

First of all, the authors would like to express thanks to reviewers, editor-in-chief, and editing staff for their special efforts, supervision, fruitful discussion, critical reviewing, and concern to improve this work. The financial support from the Deanship of Scientific Research and Graduate Studies at Yarmouk University is gratefully acknowledged

(Project number: 29/2015). Thanks are given to Prof. Dr. Ahmad Abu Hilal for his critical notes to improve this paper.

References

- Abd El-Raheem, F.H., Selim, K.A., Abdel-Khalek, N.A. (2009). Some parameters affecting beneficiation of fine kaolin particles. *The Journal of Ore Dressing* 11 (21): 1-8.
- Abedlhamid, G. (1995). *The Geology of Jarash Area*, Map Sheet 3154-I, National Resources Authority, Amman.
- Abu Hamad, A.H., Amireh, B. Jasper, A., Uhl, D. (2016). New Palaeobotanical data from the Jarash Formation (Aptian-Albian, Kurnub Group) of NW Jordan. *The Palaeobotanist* 65 (1): 19–29.
- Abu Yaya, E. K., Tiburu, M.E., Vickers, J.K., Efavi, B., Onwona A., Kevin, M.K. (2017). Characterization and identification of local kaolin clay from Ghana: A potential material for electro porcelain insulator fabrication. *Applied Clay Science* 150: 125-130.
- Ahmad, F., Abu hamad, A. Obidat, M. (2012). Palynological study of the Early Cretaceous Kurnub Sandstone Formation, Mahis area Central Jordan. *Acta Palaeobotanica* 52(2): 303-315.
- Al Ani, T. and Sarapaa, O. (2008). *Clay and Clay Mineralogy. Physical- Chemical properties and Industrial uses*. Geological Survey of Finland, Finland.
- Al-Momani, T.M. (2000). *Characterization, Industrial Utilization and Environmental Impact of the Hiswa Clay Deposits, South Jordan*. Ph.D. Thesis, University of Jordan, Jordan.
- Al-Momani, T.M. (2008). *Reducing the Iron Content of Hiswa Clay Deposits, South Jordan by Chemical Leaching*. Abhath

- AL-Yarmouk: "Basic Science and Engineering 17: 127-145.
- Al-Momani, T.M. and Dwairi, M. (2018). Physical and technical characteristics of Jarash Clay deposits from northern Jordan. *Jordan Journal of earth and environmental sciences* 9: 81-88.
- Al-Momani, T.M. and Khoury, H.N. (2010). Processing and Treatment of Hiswa Clay Deposits, South Jordan Using Hydrocyclone Separation and High Intensity Wet Magnetic Separation. *Dirasat: Pure Sciences* 37: 36-47.
- Alshaaer, M., Cuypers, H., Wastiels, J. (2002). Stabilization of kaolinitic soil for construction purposes by using mineral polymerization technique. In: Resheidat, M. (Ed.), *Proceedings of the 6th International Conference on Concrete Technology for Developing Countries*. pp: 1085-1092, Jordan.
- Amireh, B. (1994). Heavy and clay minerals as tools in solving stratigraphic problems: A case study from the Disi Sandstone (Early Ordovician) and the Kurnub Sandstone (Early Cretaceous) of Jordan. *Neues Jahrbuch für Geologie und Paläontologie. Monatshefte* 4: 205-222.
- Amireh, B. (1997). Sedimentology and Paleogeography of the regressive-transgressive Kurnub Group (Early Cretaceous) of Jordan. *Sedimentary Geology* 112: 69-88.
- Amireh, B. (2000). The Early Cretaceous Kurnub Group of Jordan: Subdivision. *Neues Jahrbuch für Geologie und Paläontologie Monatshefte* 2000: 29-57.
- Amireh, B. and Abed, A. (1999). Depositional Environments of the Kurnub Group (Early Cretaceous) in northern Jordan. *Journal of African earth Sciences* 29: 449-468.
- Attah, L.E. and Oden, I. M. (2010). Physico-Chemical Properties and Industrial Potential of some Clay Deposits in Calabar Area, South Eastern Nigeria. *Global Journal of Environmental Sciences* 9: 39-49.
- Bain, J.A. and Highly, D.E. (1978). Regional appraisal of clay resources challenge of the clay mineralogist. In: Mortland M. M. and Farmer V. C. (Eds.), *Proc. Int. Clay Conference*. Elsevier. Amsterdam.
- Bloodworth, A.J. Highley, D.E. Mitchell, G.J. (1993). *Industrial Mineral laboratory manual: Kaoline*. British Geological Survey. UK.
- Ciullo, P. (1996). *Industrial rock and their uses*, Noyes publication, USA.
- Correia, S.L., Curto, K.A. S., Hotza, D., Segadaes, A.M. (2005). Clays from southern Brazil: Physical, chemical and mineralogical characterization. *Material Science Forum* 498: 447-452.
- Djomogue, P. and Njopwovo, D. (2013). ET-IR Spectroscopy Applied For Surface Clay Characterization. *Journal of Surface Engineered Materials and Advanced Technology* 3: 275-282.
- Dominguez, E., Dondi, M., Etcheverry, R., Recio, C., Iglesias, C. (2016). Genesis and mining potential of kaolin deposits in Patagonia (Argentina). *Applied Clay Science* 131: 44-47.
- Erdemoğlu, M., Birinci, M., Uysal, T. (2020). Thermal Behavior of Pyrophyllite Ore during Calcination for Thermal Activation for Aluminum Extraction by Acid Leaching. *Clays and Clay Minerals* 68(2): 89-99. <https://doi.org/10.1007/s42860-019-00061-w>
- Ekosse, E. (2005). Fourier transform infrared Spectrophotometry and X-ray powder diffractometry as complementary techniques in characterizing clay size fraction of kaolin-ray. *Diffraction Unit. Faculty of Sciences, University of Botswana*. Botswana.
- Eletta, O.A., Aluko, F.I., Adekola, F.A. (2015). Bleaching of Nigerian kaolin by oxalic acid leaching. *Journal of chemical technology and metallurgy* 50: 623-630.
- Eslinger, E. and Peaver, D. (1988). Clay minerals for petroleum geologist and engineers. Short course no. 22th Sep. Society for Sedimentary Geology, Tulsa, U.S.A.
- Florunso, D.O., Olubambi, P., Borode, J.O. (2014). Characterization and qualitative analysis of some Nigerian clay deposits for refractory applications. *IOSR Journal of Applied Chemistry* 7: 40-47.
- Gougazeh, M., and Buhl, C.H. (2010). Geochemical and mineralogical characterization of the jabal al-harad kaolin deposit, Southern Jordan for its possible utilization. *Clay Minerals* 45: 307-314.
- Guggenheim, S. and Koster Van Gross, A.F. (2001). Baseline Studies of the Clay Minerals Society Source Clays: Thermal Analysis. *Clay and Clay minerals* 49 (5): 433-443.
- Hou, X. and Jones, T. (2000). *Inductively Coupled plasma/Optical Emission Spectrometry Encyclopaedia of Analytical Chemistry*. John Wiley and Sons Ltd, Chichester.
- Hutchison, C.S. (1974). *Laboratory handbook of petrographic Techniques*. John Wiley and sons, New-York.
- Johnston, C. (2017). Infrared and Raman Spectroscopies of Clay Minerals, In: Bergaia, F. (ED.), *Developments in Clay Science-8, Infrared Studies of Clay Mineral-Water Interactions*, Elsevier, U.S.A. pp. 288-309.
- Jovanovic, M. and Mujkanovic, A. (2013). Characterization, beneficiation and utilization of the clay from central Bosnia. 17th International research / expert conference "Trends in the development of machinery and associated technology", Istanbul, Turkey.
- Kakali, G., Perraki, T., Tsvivilis, S., Badogiannis, E. (2001). Thermal treatment of kaolin: the effect of mineralogy on the pozzolanic activity. *Applied Clay Science* 20: 73– 80.
- Kashcheev, D. and Turlova O.V. (2010). Physical-chemical properties of ceramic mix using Nizhneuvell Skoe clay. *Glass and Ceramics* 67 (5): 173-175.
- Kharbush, S., and Farhat, H.I. (2017). Mineralogy and physico-chemical properties of Wadi Badaa clays (Cairo-Suez district, Egypt): a prospective resource for the ceramics industry. *Arabian Journal of Geosciences* 10 (174): 3-10. <https://doi.org/10.1007/s12517-017-2969-1>.
- Khoury, H.N. (2002). *Clays and clay minerals in Jordan*. Publications of the Deanship of Academic Research. University of Jordan. Amman- Jordan.
- Khoury, H.N. (2006). *Industrial rocks and minerals in Jordan*. Publications of the Deanship of Academic Research. The University of Amman-Jordan.
- Khoury, H.N. (2019). Review of clays and clay minerals in Jordan. *Arabian Journal of Geosciences* 12: 706. <https://doi.org/10.1007/s12517-019-4882-2>.
- Khoury, H.N., Hodali, H., Hourani, M., Mubarak, Y., Faqir, N., Hanayneh, B., Esaifan, M. (2008). Mineral Polymerization of Some Industrial Rock and Minerals in Jordan. Publications of the Deanship of Academic Research. University of Jordan. Amman-Jordan.
- Khoury, H.N. and El-Sakka, W. (1986). Mineralogical and industrial characterization of the Batn El-Ghoul clay deposits, southern Jordan. *Applied Clay Science* 1(4): 321 - 331, 333, 335, 338, 341, 344, 347-351. [https://doi.org/10.1016/0169-1317\(86\)90009-8](https://doi.org/10.1016/0169-1317(86)90009-8).
- Kloprogge, J.T. (2017). Raman and Infrared Spectroscopies of Intercalated Kaolinite Groups Minerals. In: Bergaia, F. (Ed.), *Developments in Clay Science-8, Infrared Studies of Clay Mineral-Water Interactions*, Elsevier, U.S.A. pp. 343-410.
- Ligas, P. Uras, I. Dondi, M.M., Marsigli, M. (1997). Kaolinitic Materials from Romania (North- West Sardinia, Italy) and their Ceramic Properties. *Applied Clay Sciences* 12: 145-163.
- Madejová, J., Gates, W.P., Petit, S. (2017). IR Spectra of Clay Minerals. In: Bergaia, F. (Ed.), *Developments in Clay Science-8*.

- Infrared Studies of Clay Mineral-Water Interactions, Elsevier, U.S.A. pp. 107-149.
- Mark, U. (2010). Characterization of Ibero and Oboro Clay Deposits in Abia State, Nigeria for Refractory Applications. *International Journal of Natural and Applied Sciences* 6 (3): 296-305.
- Murray, H. (2007). *Applied Clay mineralogy: Occurrences, Processing and Application of Kaolin's, Bentonies, Palygorskite-Sepiolite, and Common Clays*. Elsevier, U.S.A.
- Poppe, L.J. Paskevich, V.F. Hathaway, J.C. Blackwood, D.S. (2001). *A laboratory Manual for X-Ray powder Diffraction*. U.S. Geological Survey, U.S.A.
- Preston, M. and Tatarzyn, J. (2013). *Mineral Processing Optimizing Plants efficiency With Attrition Scrubbers*. Yan-Tai Jin-Peng Mining Machinery Company. China.
- Qtaitat, M.A. and Al-Trawneh, I.N. (2005). Characterization of kaolinite of the Baten ElGhoul region/south Jordan by infrared spectroscopy. *Spectrochimica Acta Part A: Molecular and Biomolecular Spectroscopy* 61(7): 1519-1523. <https://doi.org/10.1016/j.saa.2004.11.008>
- Royal Jordanian Geographic Center, Jarash maps sheet (2003). 1:25.000, Amman, Jordan.
- Sandgren, M.E. Berglind, B. Modigh, S. (2015). *Basics in mineral processing handbook*, Finland.
- Sawariah, A. and Barjous, M. (1993). *Geology of Suwaylih area*. Map Sheet no.3154-II. Natural Resources Authority, Amman.
- Vaculikova, L. Plevona, E. Vallova, S. Koutnik, I. (2011). Characterization and differentiation of Kaolinites from selected Czech deposits using Infrared spectroscopy and differential thermal analysis. *Acta Geodynamica et Geomaterialia* 8(1):59-67.
- Welton, E. (2003). *SEM Petrology Atlas*. The American Association of Petroleum Geologists. Tulsa, Oklahoma, U.S.A.
- William, D. and Carter, B. (2009). *Transmission electron microscopy a textbook for materials sciences*. 2nd Ed., Springer, U.S.A.
- Yasin, S. and Ghannam, A. (2006). *Kaolinite*, National Resource Authority, Amman, Jordan.